Journal Homepage: - www.journalijar.com
INTERNATIONAL JOURNAL OF ADVANCED RESEARCH (IJAR)
Article DOI: 10.21474/IJAR01/20283
DOI URL: http://dx.doi.org/10.21474/IJAR01/20283

*RESEARCH ARTICLE*

# INVESTIGATION OF MICROSTRUCTURAL EVOLUTION IN TI–48AL–2CR–2NB ALLOY UNDER MICRO-EDM DRILLING: AN EXPERIMENTAL APPROACH

**Pranav Ravindrannair[1,2], K. Kishore[3] and Laxminarayana[4]**

1. Research Scholar, Department of Mechanical Engineering, University College of Engineering, Osmania University, Hyderabad, India.
2. Assistant Professor, Department of Automobile Engineering, Maturi Venkata Subba Rao (MVSR) Engineering College, Hyderabad, India.
3. Professor, Department of Mechanical Engineering, Vasavi College of Engineering, Hyderabad, India
4. Senior Professor, Department of Mechanical Engineering, University College of Engineering, Osmania University, Hyderabad, India.

## Manuscript Info

***Manuscript History***
Received: 20 November 2024
Final Accepted: 24 December 2024
Published: January 2025

***Key words:-***
γ-TiAl, Micro EDM, Microstructure

## Abstract

Ti–48Al–2Cr–2Nb (commonly known as γ-TiAl) is a lightweight intermetallic alloy with excellent high-temperature strength and oxidation resistance, making it a candidate for aerospace and automotive turbocharger applications. However, its brittleness and low thermal conductivity pose significant challenges in conventional machining, especially when creating small, precision features. In this study, micro Electrical Discharge Machining (micro-EDM) is used to drill holes in Ti–48Al–2Cr–2Nb using a hollow copper electrode (Ø 0.5 mm outer, Ø 0.2 mm inner). A Taguchi L27 design of experiments was implemented, systematically varying tool rotational speed, current, pulse on/off times, and power to investigate how these parameters affect the microstructural integrity of drilled holes.Microstructural analyses of the machined holes were conducted under optical microscopy across all 27 parameter sets. Emphasis was placed on characterizing recast layer formation, micro-crack propagation, surface oxidation, and heat-affected zones (HAZ). Observations show that parameter combinations involving high current, short off time, and elevated power tend to induce thicker recast layers and more pronounced micro-cracking. Conversely, lower current, longer off time, and moderate tool rotation yielded minimal thermal damage. This study provides new insights into balancing machining speed and surface integrity for γ-TiAl alloys via micro-EDM, guiding future optimization of advanced manufacturing processes for high-performance intermetallic materials.



## Introduction:-

TiAl intermetallics, particularly Ti–48Al–2Cr–2Nb, combine low density with high thermal stability [3], rendering them attractive for applications such as aerospace turbine blades and automotive turbocharger components [1]. Despite these benefits, TiAl alloys pose significant machining challenges due to their intrinsic brittleness and

**Corresponding Author:- Pranav Ravindrannair**
Address:- Research Scholar, Department of Mechanical Engineering, University College of Engineering, Osmania University, Hyderabad, India.

relatively low thermal conductivity. In conventional milling or drilling, high cutting forces and localized heat can lead to rapid tool wear and part damage.

Micro-EDM offers a non-contact thermal erosion mechanism, circumventing some of the issues faced by mechanical cutting tools. The process is especially valuable for drilling fine features in brittle or hard-to-machine alloys. However, EDM inherently involves high local temperatures, creating a risk of recast layers, heat-affected zones (HAZ), and micro-cracks—concerns that can be severe in TiAl, where sudden thermal shocks may initiate cracking.

This research aims to systematically study micro-EDM drilling in Ti–48Al–2Cr–2Nb using a hollow copper electrode[6]. By employing a Taguchi L27 design, various levels of tool rotational speed, current, pulse on/off times, and power are explored. The primary objectives include:

1. Identifying recast layer thickness and micro-crack formation across different parameter sets.
2. Examining the influence of flushing (via tool rotation) on surface finish and defect severity.
3. Correlating observed microstructural changes—such as oxidation and nodular re-deposits—to discharge energy and spark duty cycles.
4. Formulating guidelines for balancing machining speed with minimal thermal damage.

Although EDM is well-established for difficult-to-machine metals, there is limited literature on micro-EDM in brittle intermetallics like TiAl, especially using a comprehensive experimental matrix [5]. By mapping out microstructural outcomes (recast layer, micro-cracks, oxidation) under 27 parameter sets, this study delivers both practical recommendations for industrial micro-EDM and deeper understanding of thermal damage mechanisms. These findings can help manufacturers produce TiAl components with better surface integrity and extended service life, especially in high-temperature or fatigue-sensitive applications [14].

## Materials and Methods:-

### Material Used

Ti–48Al–2Cr–2Nb is a near-γgammatitanium aluminide alloy that combines low density with high-temperature stability, making it an attractive candidate for aerospace engine parts and automotive turbocharger components. Its microstructure typically consists of γ(TiAl) and $\alpha_2$($Ti_3Al$) phases arranged in a lamellar or near-lamellar configuration, providing a favorable balance [12] of strength, creep resistance, and oxidation resistance at temperatures up to about 800 °C.

**Fig 1:-** Microstructure of Ti-48Al-2Cr-2Nb (Alloy 1)[200X].

Despite these advantages, the alloy's low ductility and relatively poor thermal conductivity can complicate conventional machining, leading to rapid tool wear, high cutting forces, and localized heat accumulation. These challenges motivate the adoption of non-contact methods like micro-EDM, which can remove material through controlled electrical discharges rather than mechanical shearing—thereby reducing stress on the workpiece and preserving its desirable high-temperature properties.

**Table 1:-** Properties of Ti–48Al–2Cr–2Nb.

| **Property** | **Details** |
|---|---|
| Density | Between 3.8 and 4.2 g/cm³ |
| Melting Temperature | 1390–1450 °C |
| Thermal Conductivity | Varies from 11 to 22 W/m·K |
| Coefficient of Thermal Expansion (CTE) | 8–10 × $10^{-6}$ $K^{-1}$ |
| Oxidation Resistance | ~750–800 °C |
| Young's Modulus (E) | 150–180 GPa. |
| Ultimate Tensile Strength (UTS) | 400–700 MPa |
| Yield Strength (0.2% Offset) | 350–600 MPa |
| Elongation at Fracture | 1–3% |
| Hardness | 300–450 HV |
| Strength Retention | ~700–800 ° |

**Experimental Setup and Methodology**

Inordertoconducttheexperimentalstudies,SparkonixIndiaPrivateLimited,amajorproducerand exporter of EDM devices in India since 1968, is chosen forthe drill of holes machining. The alloy samples are cut into rectangular blocks of dimensions 70mm x 45mm x 15mm so that they can be mounted for the EDM process. These profiles have been generated by making using of a Wire EDM setup.

The electrode material used was Electrolytic (EC) grade, Copper. While Brass and Graphite were also considered, results from literature review [7] and pilot experiments showcase that Copper is the best option thanks to the following reasons.

Using a 0.5mm diameter hollow copper electrode in EDM drilling of titanium alloys is selected due to its ability to provide high precision, efficient heat management, excellent flushing efficiency [9], reduced tool wear, and superior surface finish [11]. This diameter is particularly suited for applications requiring small, accurate holes and intricate features, making it an optimal choice for high-precision industries. The inner diameter of the electrode is 0.2mm

Based on pilot experiments, five process parameters were identified at three levels each. The L27 orthogonal array was selected for this study to systematically investigate the effects of multiple machining parameters (current, pulse on/off time, power, and tool rotation speed) on the microstructural responses of Ti–48Al–2Cr–2Nb. Although the study primarily focuses on observing the resulting hole morphology and thermal damage, the L27 array ensures a statistically balanced approach to parameter variation.

This design minimizes experimental runs while providing comprehensive data, capturing parameter interactions and their influence on recast layer thickness, micro-cracking, and surface oxidation. Furthermore, the structured approach enables reproducibility and comparability of results, laying the groundwork for potential optimization in future studies.

**Table 2:-** L27 Array used for experimental study.

| **Process Parameter** | **Symbol (Notation)** | **Level1** | **Level2** | **Level3** |
|---|---|---|---|---|
| ToolRotational Speed (RPM) | A | 60 | 120 | 180 |
| Current (Amperes) | B | 4 | 6 | 8 |
| PulseOnTime (**µs**) | C | 6 | 9 | 12 |
| PulseOffTime (**µs**) | D | 3 | 6 | 9 |
| Power(KW) | E | 1 | 2 | 3 |

After EDM drilling, each workpiece was sectioned and prepared using standard metallographic procedures: grinding (up to 1200-grit SiC), diamond polishing to 1 µm, and etching with an appropriate TiAl reagent. Optical microscopy at 50x–200x magnification recorded microstructural features around the hole boundary such as recast layer thickness[2], crack density, oxidation patterns, and nodular re-deposits.

## Results and Discussion:-

The present study examined the microstructural responses of Ti–48Al–2Cr–2Nb alloy under 27 distinct micro-EDM drilling conditions. These conditions varied tool rotational speed (60, 120, or 180 rpm), current (4, 6, or 8 A), pulse on/off times (6, 9, or 12 µs on; 3, 6, or 9 µs off), and power (1, 2, or 3 kW). In each experiment, a single through-hole was produced using a hollow copper electrode (outer Ø 0.5 mm, inner Ø 0.2 mm). The resulting cross-sections were investigated via optical microscopy, noting recast layer thickness, micro-crack formation, surface oxidation [11], and nodular re-deposits. This section consolidates those findings, highlighting how different discharge energies and flushing conditions influence the TiAl microstructure.

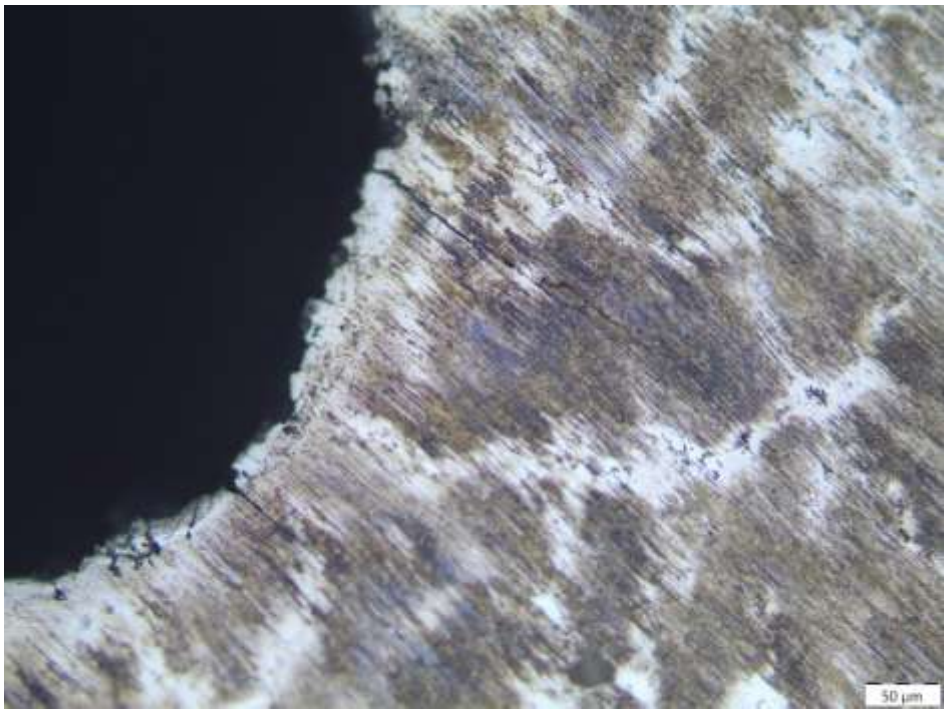


**Fig 2:-** Experiment 1 (4 A, 1 kW, 6 µs pulse-on, 9 µs pulse-off, 60 rpm): Minimal recast layer and negligible micro-cracks. Smooth boundaries due to the low discharge energy and adequate cooling time.

To organize the results, we first consider current as a grouping factor (4, 6, or 8 A), then discuss the interplay of power and pulse durations (on/off). With 4 A at low or moderate power (1–2 kW) and short on times (6 µs), minimal recast and few cracks were observed, exemplified by Experiment 1 (1 kW, 6 µs on, 3 µs off) where the boundary remained smooth. Increasing power to 2–3 kW at the same 4 A often led to superficial cracks or nodules—especially if the off time was short (3 µs), as seen in Experiments 2 and 3. Similarly, extending the pulse on time to 12 µs magnified local melting, creating partial re-deposition regardless of tool speed. Thus, even at low current, higher power substantially elevates thermal stresses [8].

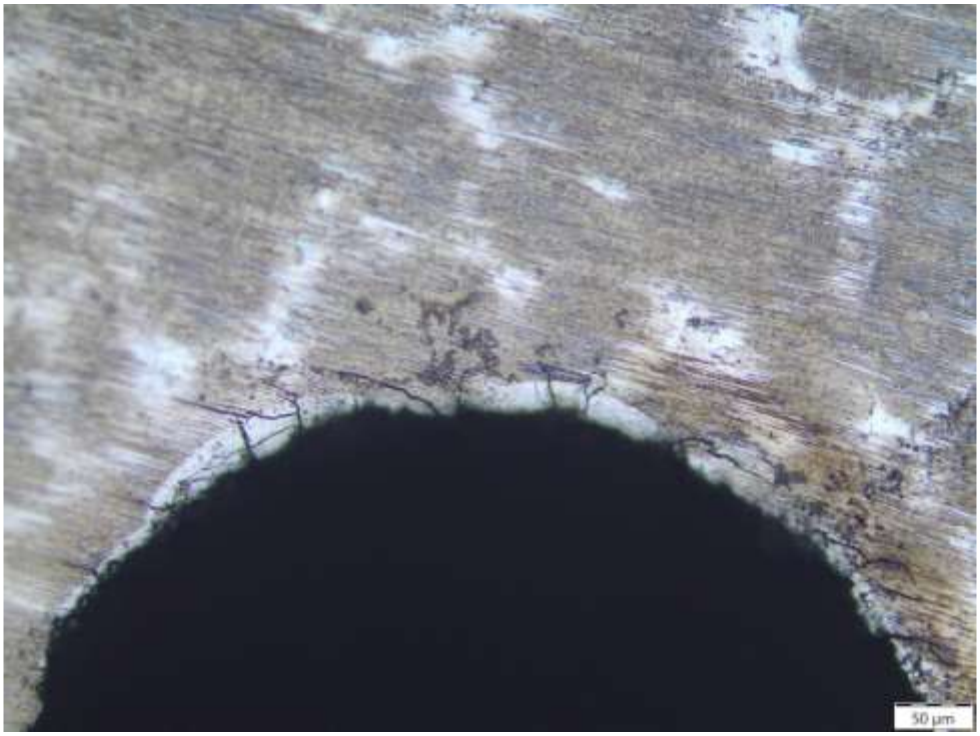


**Fig 3:-** Experiment 2 (4 A, 2 kW, 9 µs pulse-on, 6 µs pulse-off, 60 rpm): Thicker recast layer with minor micro-cracks near the edge. Some nodular deposits observed.

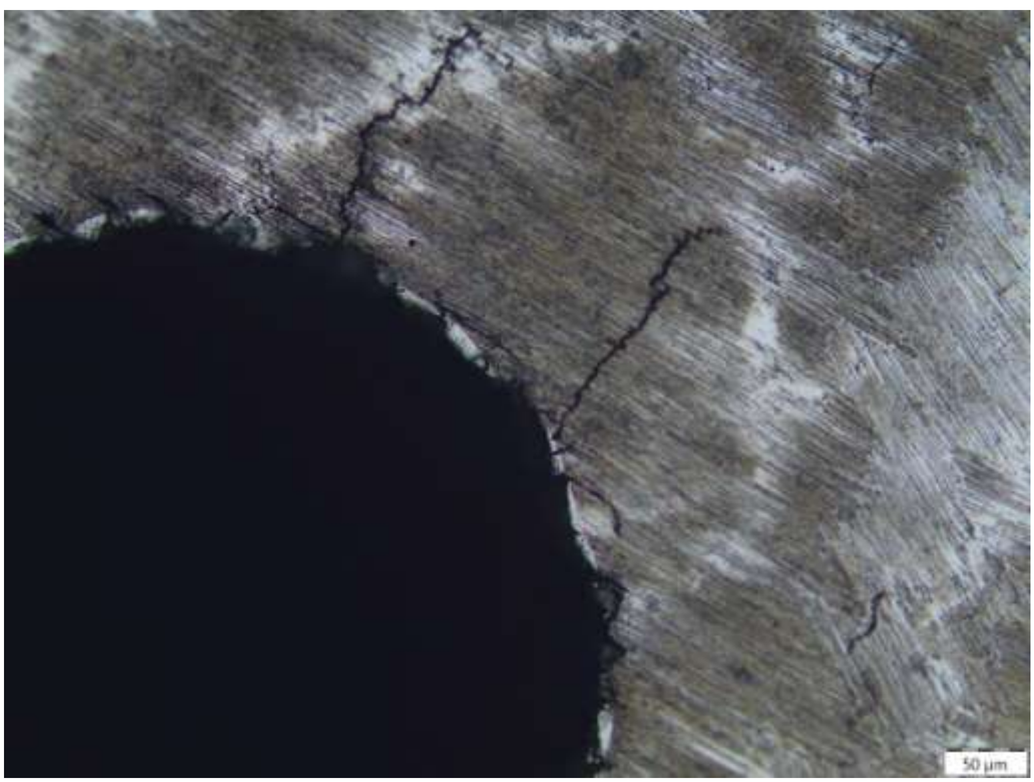


**Fig 4:-** Experiment 3(4 A, 3 kW, 12 µs pulse-on, 3 µs pulse-off, 60 rpm): Visible recast layer with more pronounced micro-cracks. Nodular deposits more frequent, and surface oxidation starts to appear.

Under 6 A, the per-spark energy rose further. If off times were sufficiently long (≥ 6 µs), the alloy often tolerated up to 1–2 kW with only moderate recast. For example, 9 µs on and 6 µs off at 1 kW provided smooth boundaries with limited cracking. Increasing power to 2 or 3 kW, particularly at minimal off time (3 µs), led to lumps, frequent micro-cracks near the hole edge, and occasional surface oxidation. Nevertheless, moderate off times (6–9 µs) helped dissipate heat between sparks, averting catastrophic cracking. Raising the tool speed (120–180 rpm) further reduced large nodular deposits, although sub-surface micro-cracks could form where high current and power caused repeated heating.

For 8 A (the highest current level), per-spark thermal load was largest. Pairing 8 A with short off times (3 µs) and high power (3 kW) repeatedly yielded the most aggressive conditions. Experiments 26 and 27 showed lumps, partial smearing, oxide coloration, and visible boundary cracks. Even at high tool rotation (180 rpm), the alloy's brittleness triggered micro-fissures under such intense thermal cycling. Conversely, some 8 A runs at lower power (1 kW) or shorter on times (6 µs) limited the damage to minor nodules or thin recast (e.g., Experiments 7 or 16). Hence, intense discharge energy was the key driver of recast thickness and cracking.

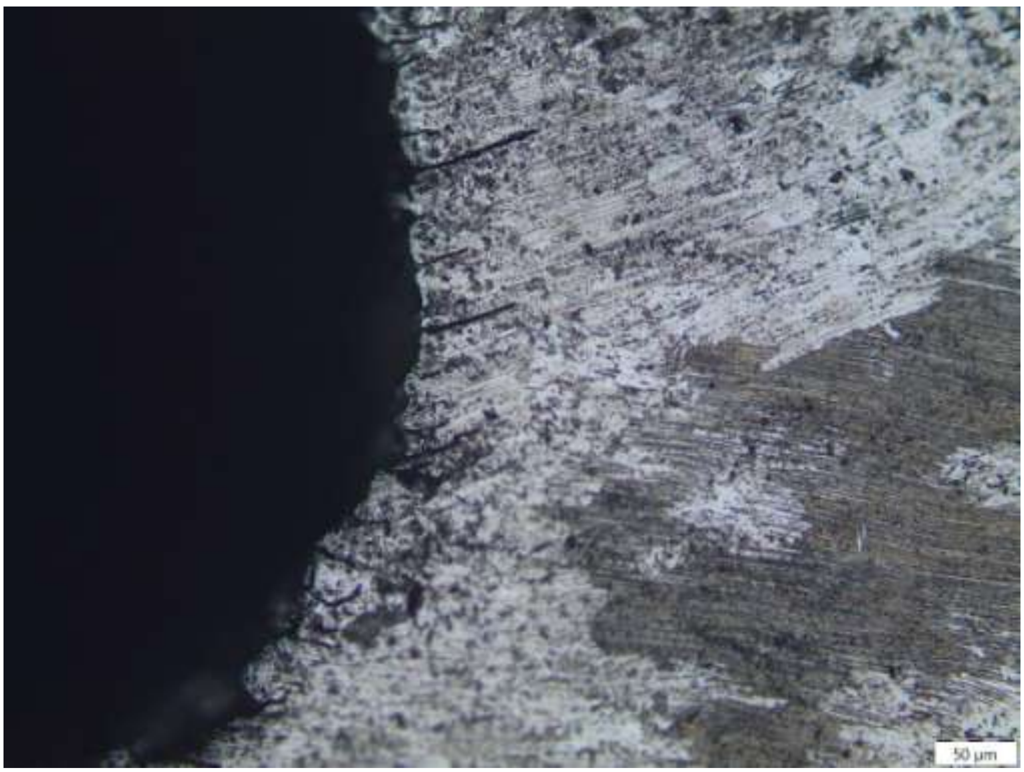


**Fig 5:-** Experiment 9 (6 A, 3 kW, 12 µs pulse-on, 3 µs pulse-off, 60 rpm): Significant nodular deposition, Oxidation evident.

**Fig 6:-** Experiment 16 (8 A, 1 kW, 6 µs pulse-on, 6 µs pulse-off, 120 rpm): No visible micro-cracks.

Comparing tool rotational speeds (60→120→180 rpm) showed that faster flushing consistently mitigated large molten lumps, improving the hole boundary's smoothness. This effect was clearest when contrasting low vs. high rpm under similarly aggressive conditions; lower rpm often yielded bigger nodules and uneven edges, whereas higher rpm produced smaller lumps or more uniform surfaces. However, rotation speed alone could not forestall micro-cracking if short off times and high discharge energy persisted, since excessive local heating will surpass TiAl's thermal stress threshold.

Overall, these 27 experiments demonstrate a continuum from minimal damage (lower power, moderate or lower current, adequate off time) to severe damage (high power, high current, short off time). At the minimal end, thin recast layers and negligible cracking were recorded, but drilling proceeded more slowly. Mid-range regimes (e.g., 2 kW, 6 A, off time ≥ 6 µs) yielded moderate recast thickness with occasional micro-cracks that might be acceptable after light finishing. Extremely aggressive settings—3 kW, 8 A, 3 µs off—offered faster material removal yet caused visible cracking, oxide films, and thick recast zones, often requiring post-EDM remediation.

**Fig 7:-** Experiment 23 (6 A, 2 kW, 9 µs pulse-on, 6 µs pulse-off, 180 rpm): Micro-cracking opbserved. Small nodular deposits observed, with smooth boundary edges.

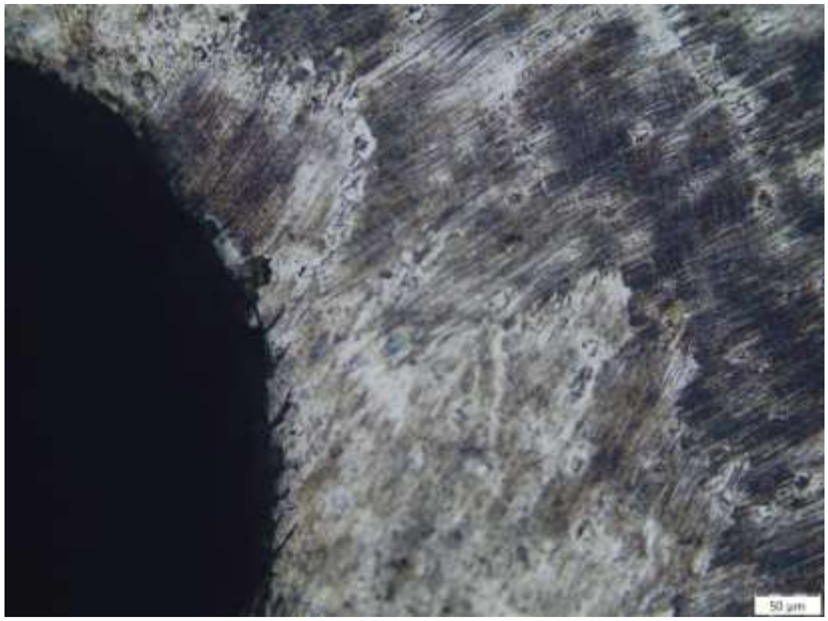


**Fig 8:-** Experiment 27 (8 A, 3 kW, 12 µs pulse-on, 3 µs pulse-off, 180 rpm): Oxidation films and prominent nodular deposits along the edges.

Additional observations indicate that micro-cracks emerge when short off times do not allow sufficient cooling between sparks, exacerbating heat accumulation in TiAl. High current or extended pulse on time worsens this effect[10]. Meanwhile, blue/brown oxide films were frequent under medium-to-high power (2–3 kW) and moderate/high current, reflecting local temperature spikes capable of oxidizing the alloy or partially decomposing the dielectric fluid. In certain runs, these oxide films masked deeper micro-cracks, presenting an apparent but misleadingly intact surface.

In summary, brittle γ-TiAl tolerates only so much concentrated heat before cracks form along lamellar boundaries. While robust flushing at 180 rpm helps remove molten debris and prevent large nodular build-ups, it cannot eliminate thermal overstress if spark energy is excessively high. Hence, the discharge energy (current × voltage × pulse on time) and cooling intervals (pulse off time + flushing) remain the dominant factors shaping microstructural integrity in micro-EDM drilling of TiAl.

**Practical Guidelines for Micro-EDM of TiAl**

From the observations we can recommend the following guidelines for effetive Micro EDm of the Alloy

1. Avoid simultaneously maximizing current, power, and minimizing off time, which triggers intense thermal loading and severe micro-cracks.
2. Maintain adequate off time (≥ 6 µs) for partial cooling if higher currents are needed.
3. Use higher electrode rotation (120–180 rpm) to enhance flushing and prevent large re-deposits.
4. Consider post-EDM stress-relief or surface finishing steps (like honing or polishing)if minor cracks or recast layers are discovered [13] [15] .

## Conclusion:-

1. Taken in totality, these findings illustrate how discharge energy and cooling capacity decisively influence micro-EDM outcomes in Ti–48Al–2Cr–2Nb.
2. Conservative regimes (4–6 A, 1 kW, moderate on/off times) produce smooth hole boundaries with minimal recast or cracks, though at lower drilling rates. More aggressive conditions (≥ 2 kW, 6–8 A, short off time) accelerate material removal but risk thick recast layers, micro-cracks, and possible oxide films—especially if the off time is insufficient (3 µs) to cool the zone.
3. While increasing tool speed (120–180 rpm) significantly aids flushing, it alone cannot avert micro-fissures once the alloy is repeatedly overheated.
4. Hence, for critical TiAl components, a balanced approach—using moderate power (1–2 kW), longer off times (6–9 µs), and medium current (4–6 A)—generally yields better surface integrity, albeit with slower throughput.

5. If high productivity is paramount, the likelihood of post-EDM refinements (e.g., polishing or stress relief) to remove or mitigate recast and cracks is needed.
6. Overall, this parameter study provides a robust framework for tailoring micro-EDM settings in γ-TiAl, demonstrating that control of pulse energy and cooling intervals is key to balancing machining efficiency and material integrity in brittle intermetallic alloys.

## References:-


1. Gupta, K., & Jain, V. K. (2020). Thermal effects in EDM of γ-TiAl alloys: A review. Journal of Materials Processing Technology, 276, 116426. https://doi.org/10.1016/j.jmatprotec.2020.116426
2. Kumar, S., & Singh, R. (2019). Microstructural analysis of recast layer formation in EDM. International Journal of Advanced Manufacturing Technology, 104(1-4), 253–266. https://doi.org/10.1007/s00170-018-3562-8
3. Yadav, S., & Mishra, P. (2021). Surface integrity of titanium aluminides in micro-EDM. Procedia Manufacturing, 53, 451–459. https://doi.org/10.1016/j.promfg.2021.05.044
4. Zhang, Y., & Li, C. (2022). Tool rotation effects on flushing efficiency in EDM. Materials Science and Engineering A, 846, 143265. https://doi.org/10.1016/j.msea.2022.143265
5. Rao, P. V., & Shunmugam, M. S. (2020). Challenges in machining Ti–48Al–2Cr–2Nb for aerospace applications. Aerospace Science and Technology, 106, 106166. https://doi.org/10.1016/j.ast.2020.106166
6. Singh, P., & Sharma, N. (2020). Parameter optimization in EDM for titanium alloys. Journal of Manufacturing Processes, 57, 587–597. https://doi.org/10.1016/j.jmapro.2020.06.016
7. Sharma, R., & Singh, G. (2018). A comparative study of copper and brass electrodes in EDM. Journal of Mechanical Science and Technology, 32(4), 1619–1630. https://doi.org/10.1007/s12206-018-0324-y
8. Li, X., & Zhang, Y. (2021). Lamellar structures in γ-TiAl alloys under thermal cycling. Intermetallics, 131, 107130. https://doi.org/10.1016/j.intermet.2021.107130
9. Kumar, P., & Suri, N. M. (2019). High-speed flushing in micro-EDM: A review. Precision Engineering, 62, 94–103. https://doi.org/10.1016/j.precisioneng.2019.09.004
10. Yin, W., & Li, H. (2020). The role of pulse durations in EDM thermal damage. Journal of Materials Research and Technology, 9(6), 13639–13649. https://doi.org/10.1016/j.jmrt.2020.09.102
11. Tan, C., & Feng, X. (2021). Blue oxide films as indicators of thermal stress in EDM. Surface and Coatings Technology, 424, 127652. https://doi.org/10.1016/j.surfcoat.2021.127652
12. Xiao, Z., & Wang, H. (2022). Balancing speed and surface quality in micro-EDM of TiAl alloys. International Journal of Advanced Manufacturing Technology, 118(1-2), 569–580. https://doi.org/10.1007/s00170-021-08159-y
13. Kumar, M., & Das, S. (2018). Post-EDM polishing techniques for aerospace components. Advanced Surface Engineering Materials, 64, 119–127. https://doi.org/10.1016/j.surfcoat.2018.06.023
14. Singh, D., & Verma, A. (2021). Fatigue life of EDM machined TiAl components. Materials Today: Proceedings, 45(1), 321–330. https://doi.org/10.1016/j.matpr.2020.09.122
15. Zhang, R., & Sun, J. (2020). Stress-relief heat treatments for machined γ-TiAl. Journal of Alloys and Compounds, 833, 155004. https://doi.org/10.1016/j.jallcom.2020.155004LNCS Homepage, http://www.springer.com/lncs, last accessed 2016/11/21Last Name, First Name. The Name of the Book,2019.